Drilling into the metabolomics to enhance insight on corn and wheat responses to molybdenum trioxide nanoparticles

Xiangning Huang[‡], *Pabel Cervantes-Avilés*[§ ‡], *Weiwei Li*[†], *and Arturo A. Keller*[† ‡*]

[†] Bren School of Environmental Science and Management, University of California at Santa Barbara, CA, USA 93106

[‡] University of California, Center for Environmental Implications of Nanotechnology, Santa Barbara, CA, USA 93106

[§] Tecnológico de Monterrey, Escuela de Ingeniería y Ciencias, Puebla, México CP 72453

Corresponding author: Tel: +1 805 893 7548; fax: +1 805 893 7612.

Email address: arturokeller@ucsb.edu

Graphic for Table of Contents

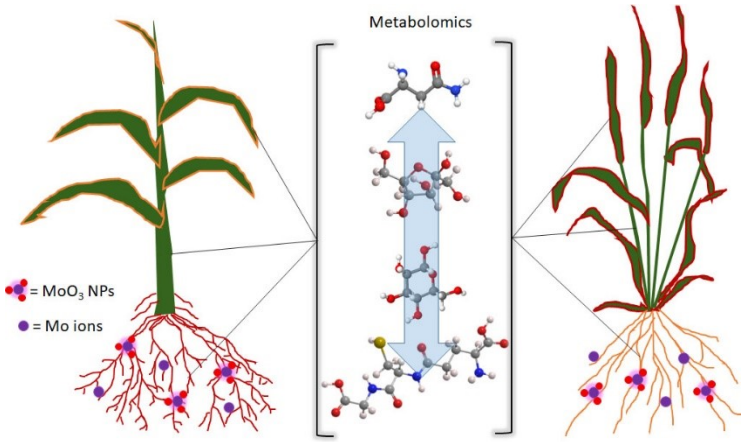

Abstract

Metabolomics is an emerging tool to understand the potential implications of nanotechnology, particularly for agriculture. Although molybdenum (Mo) is a known plant micronutrient, little is known of its metabolic perturbations. Here, corn and wheat seedlings were exposed to MoO_3 nanoparticles (NPs) and the corresponding bioavailable Mo^{6+} ion at moderate and excessive levels through root exposures. Physiologically, corn was more sensitive to Mo, which accumulated up to 3.63 times more Mo than wheat. In contrast, metabolomics indicated 21 dysregulated metabolites in corn leaves and 53 in wheat leaves. Five more metabolomic pathways were perturbed in wheat leaves compared to corn leaves. In addition to the overall metabolomics analysis, we also analyzed individual metabolite classes (e.g., amino acids, organic acids, etc.), yielding additional dysregulated metabolites in plant tissues: 7 for corn and 7 for wheat. Most of these were amino acids as well as some sugars. Additional significantly dysregulated metabolites (e.g., asparagine, fructose, reduced glutathione, mannose) were identified in both corn and wheat, due to Mo NP exposure, by employing individual metabolite group analysis. Targeted metabolite analysis of individual groups is thus important for finding additional significant metabolites. We demonstrate the value of metabolomics to study early-stage plant responses to NP exposure.

Keywords: nanofertilizer, nanoagriculture, micronutrient, bioaccumulation, uptake

Synopsis

Greater insights can be obtained by an in-depth analysis of the changes in metabolite levels due to exposure of plants to nanomaterials, such as MoO_3 nanoparticles

Introduction

Metabolomics is emerging as a very important tool for elucidating the potential benefits and risks of employing nanomaterials (NMs) to enhance agricultural production [1]. It is in the past few years that metabolomics has risen as an important tool in crop production enhancement [2–6]. Determining the up- or down-regulation of metabolites as a function of NM exposure can serve to evaluate hypotheses regarding the expected improvement in crop yield, or unexpected changes in nutritional value, plant health or other outcomes. One of the major advantages of metabolomics relative to traditional toxicology is that changes in metabolite levels can be detected at lower, more realistic exposure concentrations.

NMs have been proposed for use as nanofertilizers [7], nanopesticides [8] and even nanosensors [9]. Compared with conventional agrochemicals, nanofertilizers and nanopesticides may have 20-30% higher efficacy in delivering the target active ingredient (nutrients or pesticides), which could substantially reduce the use of agrochemicals [10]. Molybdenum (Mo) is an essential micronutrient required for growth of most plants [11], mainly accessible to plants as MoO_4^{-2} [7,12–16]. Mo usually participates in reductive and oxidative reactions in plants via specific plant enzymes [14]. Mo plays an important role in N fixation in legumes, and in regulation in other plants of nitrate reduction, as well as amino acid and protein biosynthesis [11]. Application can be approximately 0.5 kg/ha, requiring careful dosing [17]. While the role of molybdenum in plant growth is indeed significant, studies on the applications of nano-MoO_3 as micronutrient and/or

56 promotor of plant growth are rather limited [1,18-22]. Applications at the nanoscale may result in more effective
57 dosing. Thus, studies on the accumulation and uptake of Mo and Mo oxide nanoparticles have been
58 conducted on various plant species, such as maize (*Zea mays* Weike720) [23], rice (*Oryza sativa L.*) [18, 22],
59 cowpeas (*Vigna unguiculata*) [19], potato (*Solanum tuberosum L.*) [20], and spinach (*Spinacia oleracea L.*) [21].
60 However, excess Mo NPs exposure can inhibit root growth/elongation, prolong seed germination, increase
61 nitrate reductase, and cause oxidative imbalance [18-22]. While it is useful to study the physiological response
62 of plants to Mo NPs, a molecular level examination of the effect of Mo NPs is needed. Thus, metabolomics
63 is a useful tool to explore the response of crop plants to Mo NPs.

64 Metabolites are the end products of cellular regulatory processes; monitoring metabolite changes at
65 the molecular level in plant tissues enhances the information provided by physiological measurements [23].
66 For example, the physiological data from a study conducted by Olkhovych et al. (2018) showed that Zn
67 NPs resulted in discoloration of *Pistia stratiotes L.* leaves, but this was not the case for Cu NPs [24]. In
68 contrast, levels of eight amino acids were significantly altered after Cu NP exposure but only five amino
69 acids were dysregulated after Zn NP exposure [24]. Amino acids can act as metal-chelators, signaling
70 molecules, and antioxidant agents during plant defense reactions [25]. The changes in amino acid levels
71 illustrate the adaptive ability of plants under environmental stress. Another metabolomics study employed
72 liquid chromatograph-mass spectrometry (LC-MS) to analyze changes in polyphenol levels in cucumber
73 leaves exposed to copper [26]. Even though leaf biomass remained unchanged for all applied concentrations
74 (i.e., 0.21, 2.1, and 10 mg Cu/plant), the levels of some polyphenol compounds (e.g., N-acetyl-L-methionine
75 and N-acetyltyptophan) exhibited a significant change even when copper dose was as low as 0.21 mg
76 Cu/plant. N-acetyl-L-methionine is a superior reactive oxygen species (ROS) scavenger and N-
77 acetyltyptophan can prevent protein molecules from oxidative degradation.

78 Metabolomics studies can be untargeted or targeted. Untargeted metabolomics studies serve for a
79 broad, semi-quantitative assessment of the changes in hundreds or thousands of metabolites due to a
80 particular exposure [1], and are useful for generating hypotheses. They are semi-quantitative, since standards

are not used to accurately quantify the changes in metabolite levels in plant tissues as a function of the exposure to stressors such as NPs. There are several recent untargeted metabolomics studies on the effects of NMs on plants [27–34]. For example, by studying the metabolic responses of corn (*Zea mays*) leaves to $Cu(OH)_2$ NPs through leaf exposures, Zhao et al. (2017) discovered that a dose of 100 mg of $Cu(OH)_2$ NPs per plant significantly increased phenylalanine (23.9%), tyrosine (39.5 %), and 4-hydroxycinnamic acid (121.9%) [29]. Several pathways were perturbed (e.g., glycolysis pathway, tricarboxylic acids cycle (TCA), and shikimate-phenylpropanoid biosynthesis) indicating the activation of energy metabolism and plant defense processes [30]. In another study, foliar application of Ag NPs and Ag ions to cucumber (*Cucumis sativus*) leaves indicated that phytol was significantly increased (1.5-2.2-fold) and implicated the degradation of the photosynthesis process [32]. In addition, the significant upregulation of antioxidants (arbutin and salicin) and aromatic compounds (4-hydroxyquinazoline, 3-hydroxybenzoic, acid, 1,2,4-benzenetriol, and pyrogallol) demonstrated the activation of plant defense systems (i.e., triggered by the overproduction of reactive oxygen species (ROS)). However, due to the semi-quantitative nature of the untargeted metabolomics and challenges in detecting less abundant compounds, subtle yet statistically significant changes in metabolite levels may remain hidden.

Targeted metabolomics provide a more rigorous quantitative approach, which can serve to test hypotheses, albeit usually considering a smaller number of metabolites [35–39]. Calibration with isotopically-labelled internal standards is used for absolute quantitation of the target metabolites. In addition to calibration curves for each metabolite, the recovery of each metabolite from the plant tissue is also determined, which is an important factor in the overall analysis. Huang et al. (2018) conducted a systematic study of plant tissue (cucumber leaves) extraction and LC-MS/MS optimization for 23 amino acids [36]. The high sensitivity (limit of detection as low as 0.005 ng/ml) and high recovery rates (80-120%) proved the precision and accuracy of targeted analysis. In addition, the levels of many amino acids in cucumber leaf tissues exposed to Cu NPs were significantly altered. In another recent study, targeted metabolomics was employed to study algae exposed to Ag NPs; 94 metabolites were considered, including amino acids,

106 nucleobases/sides/tides, amines, antioxidants, organic acids/phenolics, sugars/sugar alcohols and fatty acids
107 [38]. These metabolites were selected after a preliminary analysis with untargeted metabolomics revealed that
108 these were the most dysregulated. Ag NPs were shown to affect amino acid metabolism, TCA cycle, and
109 oxidative stress. An analysis of the overall response indicated that 52 metabolites were responsible for the
110 discrimination between control and treatments, and 45 dysregulated metabolites could be identified.
111 Similarly, a targeted metabolomics study of soybean shoots exposed to quantum dots with a similar set of
112 targeted metabolites identified 23 perturbed metabolites in the roots and 26 in the leaves [35]. In both cases,
113 the statistical analysis was performed on the entire set of metabolites, to identify the metabolites responsible
114 for the separation between control and treatments, and then characterize the metabolites that are more
115 distinctly dysregulated. Statistical evaluation of all the detected metabolites is the conventional approach
116 in both untargeted and targeted metabolomics. However, the natural concentrations of different groups of
117 metabolites can vary over orders of magnitude, such that the dysregulation (i.e., up-regulated or
118 accumulated, or down-regulated or depleted) of much less abundant yet important metabolites may be
119 undetected. We hypothesize that an analysis of the metabolites by groups can reveal more information and
120 add more value than the conventional (overall) analysis.

121 For this study, corn (*Zea mays* 'Golden Bantam') and wheat (*Triticum spp.* 'Red Fife') were selected,
122 since they are major cereal crops, to study the effect of root exposure to various levels of Mo NPs and the
123 corresponding ionic Mo concentrations. In addition to a targeted metabolomics study, we considered
124 physiological effects, changes in nutrient uptake, and Mo uptake and translocation, to relate the metabolic
125 changes to actual exposure levels. Furthermore, groups of metabolites were also statistically analyzed to
126 extract additional information on dysregulated metabolites. This work provides valuable information on
127 early-stage plant responses to Mo NPs at the molecular level, and a more comprehensive metabolite data
128 analysis approach for future metabolomics studies.

129 **Materials and methods**

130 *Characterization and stability of MoO_3 NPs*

131 MoO_3 NPs were purchased from U.S. Research Nanomaterials, Inc. (US3330) with primary particle
132 size in a range of 13 - 80 nm. NP morphology was characterized by transmission electron microscopy
133 (TEM) (FEI Tecnai G2). Surface bonding characteristics of MoO_3 NPs and the phase/crystalline structure
134 were characterized by X-ray photoelectron spectrometry (XPS, Thermo Scientific, ESCALAB 250 XI^+)
135 and X-ray diffraction (XRD) spectrum (Panalytical Empyrean Powder). The hydrodynamic diameter and
136 the surface charge (zeta potential) of MoO_3 NPs in 10% Hoagland water were measured via dynamic light
137 scattering (Zetasizer Nano ZS, Malvern) at 100 and 500 mg/L levels. Diluted Hoagland water (Table S1)
138 was employed throughout the study to provide sufficient nutrients for plant growth. A molybdenum ionic
139 salt ($Na_2MoO_4 \bullet 2H_2O$, ≥99 %) was purchased from Sigma-Aldrich and the concentrations used in the
140 treatments were determined from the stability/dissolution experiments of the MoO_3 NPs as described below.

141 Suspension stability was evaluated in the 10% Hoagland water solution at 100 and 500 mg/L. Before
142 the stability test, NP suspensions were sonicated for 30 min and distributed into three 50 ml metal-free
143 polypropylene tubes. After 2 min of vigorously vortexing, 2 ml of aliquot was withdrawn at 0 h, 6 h, 24 h,
144 72 h, 120 h, and 168 h time intervals. The suspensions were then placed in Amicon Ultra 3KDa cutoff
145 centrifugal filters (Sigma-Aldrich, UFC800324), centrifuged at 5000 rpm for 20 min, and the acidified
146 solutions were diluted 10 times for further analysis [35]. The target metal ion (i.e., Mo) was measured by
147 inductively coupled plasma-mass spectrometry (ICP-MS) (Agilent 7900, Agilent Technologies).

148

149 *Corn and wheat growth and exposure conditions*

150 Corn and wheat were selected for this study, since they are important cereal crops. Before the
151 germination procedure, all seeds were sterilized with 1% sodium hypochlorite solution for 10 min, followed
152 by rinsing 10 times with deionized water. Then the treated seeds were soaked in NANOpure water for
153 another 24 hr before germinating in water-saturated vermiculite. Vermiculite was used throughout the study

154 to obtain the desired drainage and avoid accumulation of metals and nutrients. After 7 d, seedlings were
155 transplanted to obtain two wheat seedlings per pot and one corn seedling per pot for the exposure test.

156 Before transplanting the plants for the root exposure experiments, vermiculite was mixed with
157 predetermined levels of NP suspensions or ionic solutions, and then was placed into individual pots. No
158 molybdenum was added to the control group. For the experimental groups, 40 g of vermiculite were mixed
159 with 80 ml of MoO_3 NP suspensions or ionic Mo solution before the plant exposure assay. The MoO_3 NP
160 suspensions, with concentrations of 100 and 500 mg/L, were sonicated for 30 mins and mixed with the pre-
161 weighted vermiculite to reach 200 and 1000 mg metal (Mo) content per kg of vermiculite. These doses
162 were selected based on literature values [17] for Mo requirements as well as preliminary experiments to
163 determine observable positive effects and excessive dosing. Background concentrations of Mo in
164 agriculture soils generally range from 0.2 – 5.0 mg/kg [40], however, in mining affected soils, Mo level can
165 reach up to 2903.91 mg/kg [41]. The selected doses in the current study were in the range as moderate and
166 excessive Mo levels, and they were also comparable with other Mo NPs toxicity studies on plant species [18-
167 20, 22]. Based on a related study on the dissolution and aggregation of several metal oxide NPs [42], including
168 the MoO_3 NPs used in this study, we determined the concentrations for the ionic Mo treatments
169 corresponding to the level of dissolved metal ions expected in the media, 35 and 225 mg/L Mo, to achieve
170 a bioavailable Mo comparable to the NP treatments.

171 Treated plants were grown under a 16 h photoperiod (light intensity 150 $\mu mol \cdot m^{-2} \cdot s^{-1}$) for three weeks
172 at 22 ºC and a relative humidity of 60 %. Plants were watered every day to maintain the vermiculite water
173 content between 70-90 %. Each exposure condition had a minimum of three replicates.

174

175 *Metal content accumulation and distribution*

176 Plant roots were rinsed with deionized water to eliminate vermiculite loosely adhered to the roots,
177 followed by 20 min. soaking and three times rinsing with NANOpure water [43]. Before freeze-drying, plants

178 were cut and separated into roots, shoots and leaves, and the length and fresh weight was recorded. The
179 tissues were freeze-dried and stored at -80 ºC until needed. For the analysis, freeze-dried tissues were cut
180 into small pieces and placed in 50 ml digestion tubes. Then, 2 ml of plasma pure HNO_3 was added into the
181 tube and the system was heated at 115 ºC for 20 min on an SCP Science SigiPREP hot block digestion
182 system. Then 8ml of H_2O_2 (HNO_3:H_2O_2=1:4) was added and continued to heat for another 60 min at 115
183 ºC [39, 44]. At the end of the digestion process, the digests were diluted to 50 ml with NANOpure water. The
184 acidified solutions were further diluted 10 times prior to analysis via ICP-MS (Agilent 7900, Agilent
185 Technologies). Along with the target metal ions (i.e., Mo), other macro-nutrients (i.e., Ca, K, Mg, and P)
186 and micro-nutrients (i.e., Cu, Fe, Mn, and Zn) were also quantified via the ICP-MS analysis.

187 *Metabolites extraction and LC-MS analysis*

188 After harvesting and processing, another set of plant tissues was cut and separated into roots, shoots
189 and leaves, and then immediately freeze-dried. After freeze-drying, the samples were ground into a fine
190 powder in liquid nitrogen. The samples were stored in 2-ml Eppendorf micro-centrifuge tubes at -80ºC
191 freezer before further analyses. The metabolite extraction process followed previous studies [24,35,37]. Briefly,
192 weighted 10-20 mg of frozen, finely ground plant tissue was extracted with 1 ml of 80% methanol/2%
193 formic acid in the 2 ml Eppendorf micro-centrifuge tubes. The tubes were vortexed at 3,000 rpm, sonicated,
194 and centrifuged at 20,000g for 20 min at each step. The supernatant was transferred into vials for detection
195 and quantification of amino acids, antioxidants, fatty acids, nucleobase/side/tides, organic acids/phenolics,
196 and sugar/sugar alcohols using an Agilent 1260 UHPLC binary pump coupled with an Agilent 6470 triple
197 quadrupole mass spectrometer (LC-MS/MS). The 82 selected metabolites were based on previous
198 untargeted and targeted metabolomics studies that indicated these metabolites can experience significant
199 dysregulation after NP exposure and play important roles in key metabolic pathways [26-38]. Data were
200 processed with the Agilent MassHunter Workstation Software Quantitative Analysis (V.B.07.01). The
201 detailed sample preparation, instrument settings, and running parameters are listed in the Supporting
202 Information.

203 *Statistical analysis*

204 One-way analysis of variance (ANOVA) tests followed by a Fisher's least significant
205 difference method were conducted to identify significant changes between control and the various
206 treatments, for each plant species. More specifically, the physiological parameters, mineral
207 nutrient, and metabolite levels were analyzed using SPSS Statistics 22, with the significant
208 threshold (*p-value*) set at 0.05.

209 The metabolomics statistical analysis was performed using MetaboAnalyst 5.0
210 (https://www.metaboanalyst.ca/). To set features to be more comparable, before the multivariate
211 statistical analysis, the data were normalized by sum and a log transformation. A supervised
212 particle least-squares discriminant analysis (PLS-DA) was conducted to maximize the separation
213 between control and experimental groups, which has been widely adopted in the previously similar
214 studies [25, 37, 38]. The importance of a given variable was determined by the variable importance in
215 projection (VIP), derived from the PLS-DA, considering VIP scores ≥ 1. The metabolites
216 identified as significant were derived from both the overall and sub-category metabolites.
217 Metabolite pathway analysis was performed by using MetaboAnalyst 5.0, where the impact value
218 threshold was set at 0.1 for identification of perturbed pathways.

219 **Results and discussion**

220 ***Characterization of MoO_3 NPs and the stability in the solution.***

221 Both the original MoO_3 NPs powder and the nanoparticle suspensions were characterized at the applied
222 conditions (Figure 1). As shown in the TEM image, the original MoO_3 NPs were largely spherical with a
223 diameter 30-60 nm (Figure 1A). The XRD spectra demonstrated that the MoO_3 NPs exhibit an
224 orthorhombic crystalline structure associated to the alpha (α) mineral phase. Furthermore, XPS revealed a
225 primary peak of Mo 3d located at 230.9 eV, indicating Mo was bonded to oxygen in the upper energy levels;

226 no carbon-based coating was detected (Fig 1B and 1C). For the MoO_3 NPs suspensions in 10% Hoagland
227 media at 100 and 500 mg/L, the hydrodynamic diameter ranged from 375.7 ± 18.7 nm to 399.5 ± 7.3 nm
228 and the zeta potentials from -32.0 ± 2.1 to -32.8 ± 1.2 mV, with little difference between NP concentration
229 levels. However, dissolution was a strong function of NP concentration, with a very rapid release of Mo
230 ions even at the beginning of the dissolution test (Figure 1D). At time 0, dissolution (free Mo ion) was
231 30.5% for the 100 mg/L suspension and 43.5% for the 500 mg/L suspension. Minor changes were observed
232 after 7 days, with an additional 4.5% and 4.1 % dissolution for the lower and higher MoO_3 NP levels,
233 respectively. This result was comparable with a recent study where the dissolution rate of 100 mg/L MoO_3
234 NPs was 35% at time 0 and 39% on day 6 in DI water [42]. However, when rice seedlings were immersed in
235 a Hoagland water solution the MoO_3 NP dissolution rate decreased significantly to around 10% [22]. Based
236 on the dynamic dissolution behavior of MoO_3 NPs, 35 and 225 mg/L Mo were chosen as the comparable
237 ionic Mo concentrations corresponding to 100 and 500 mg/L MoO_3 NP suspensions, respectively.
238

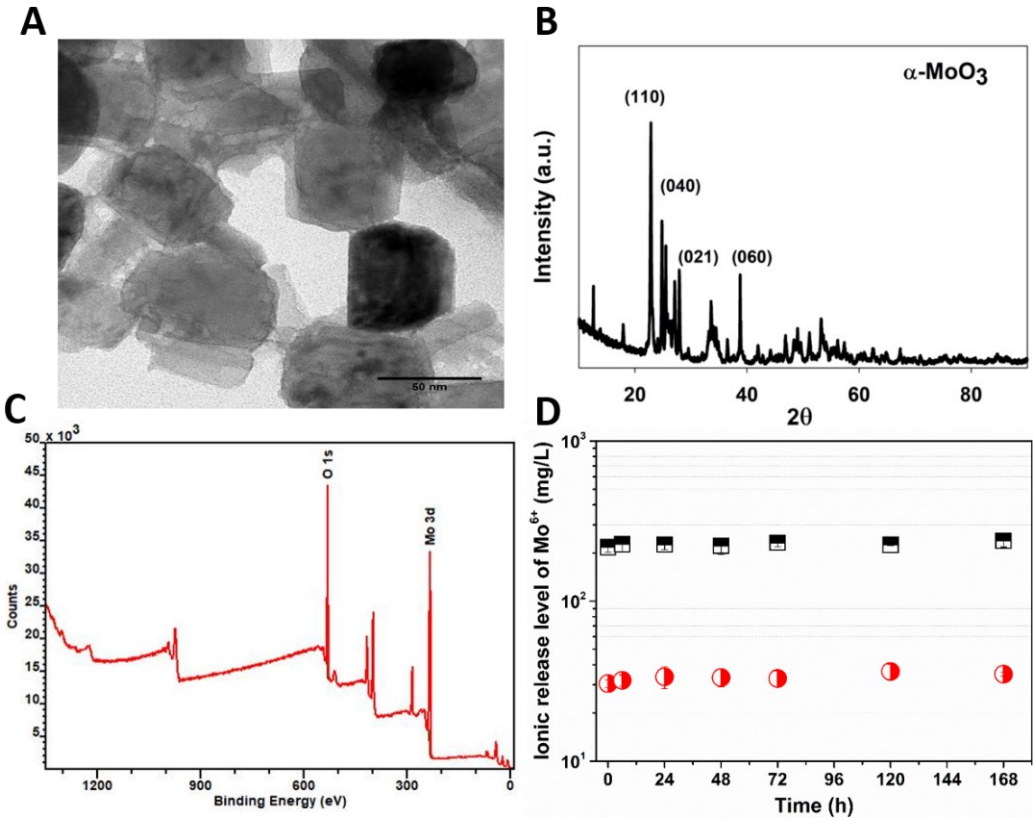

239

240 **Figure 1.** Characterization of MoO_3 NPs. (A) transmission electron microscope (TEM) imaging, (B) X-ray
241 diffraction (XRD) pattern and h-k-l reference peaks, (C) X-ray photoelectron spectroscopy (XPS) spectra,
242 and (D) ions released in 10% HA solution from MoO_3 NPs at ◑ 100 mg/L and ▬ 500 mg/L.
243

244 ***Physiological response and metal accumulation***

245 Root morphology was significantly altered, with inhibited root growth and development of lateral roots,
246 when corn and wheat were exposed via the roots to MoO_3 NPs at 200 mg/kg (treatment b) and 1000 mg/kg
247 (treatment d) compared to the control (treatment a) (Figure 2A). The effect was more pronounced for corn
248 seedlings, and at 1000 mg/kg NPs (treatment d). Exposure to the NPs at these concentrations also
249 significantly reduced root dry biomass (Figure 2B), particularly for treatment d with a 58% decrease in root
250 biomass. There was no noticeable effect for treatment c (70 mg/kg ionic Mo), whereas treatment e (450
251 mg/kg ionic Mo) did result in a significant decrease in root biomass for both corn and wheat. The decrease
252 in root biomass correlated well with Mo content in the roots (Figure 2C), where the control group
253 accumulated less than 0.001 mg Mo/g dry mass, but accumulation increased to 3.5 and 11.2 mg/g in corn
254 roots exposed to 200 and 1000 mg/kg NPs, respectively. The corresponding ionic exposure treatments (c
255 and e) accumulated 1.7 and 6.9 mg/g , which is 47% and 59% of the comparable NPs treatments. Wheat
256 accumulated 21.7-68.9 % as much Mo as corn, from either the NP exposures or the ionic Mo solutions. As
257 expected, the higher Mo dose resulted in more pronounced changes (Table S2). Uptake of Mo resulted in
258 increased uptake of Fe in corn roots, for all treatments (Figure 2D). For wheat, this only was significant for
259 the high level (1000 mg/kg NPs and 450 mg/kg ionic) treatments. There was a 55% decrease in wheat root
260 biomass for 1000 mg/kg NPs (treatment d). However, uptake of Mo resulted in decreased uptake of Zn in
261 both corn and wheat, for almost all treatments, although more pronounced for the high-level treatments.
262 This is an important concern, since lower Zn levels may affect the nutritional value of these crops.
263 Insufficient supply of vitamins and micronutrients (e.g., Zn and Fe) from food commodities (e.g., wheat)
264 affects about two billion people worldwide [46].

265 Exposure to Mo via the roots, either as NP or ionic, also affected above ground physiological responses and
266 metal accumulation/translocation (Figure 3). The first true leaves of corn exposed to Mo, particularly at
267 high levels, began to yellow and exhibit signs of senescence; wheat seedlings appeared to be less impacted
268 (Figure 3A). Exposure had a negative effect on above-ground biomass, with a significant decrease in stem
269 (up to 57%) and leaf biomass (up to 61%) for corn exposed to the 1000 mg/kg NPs (treatment d) and 450
270 mg/kg ionic (treatment e). The biomass of wheat stem and leaf was less affected, moreover, there was a
271 statistically significant increase (14%) in stem biomass for the 450 mg/kg ionic (treatment c). There was
272 significant translocation of Mo from the roots to stems and leaves, which was more pronounced for the NP
273 treatments than the corresponding ionic Mo treatments (Figures 3C and 3D), where 1.6-3.0 times more Mo
274 was translocated to plant leaves than stems. Under the same experimental conditions, corn translocated
275 1.10-1.36 times more Mo into leaf tissues than wheat. This result likely explains the earlier leaf morphology
276 alterations observed for corn leaves. Excessive application of nanosized octahedral hexamolybdenum
277 clusters also greatly inhibited rapeseed (*B. napus*) growth [44].
278

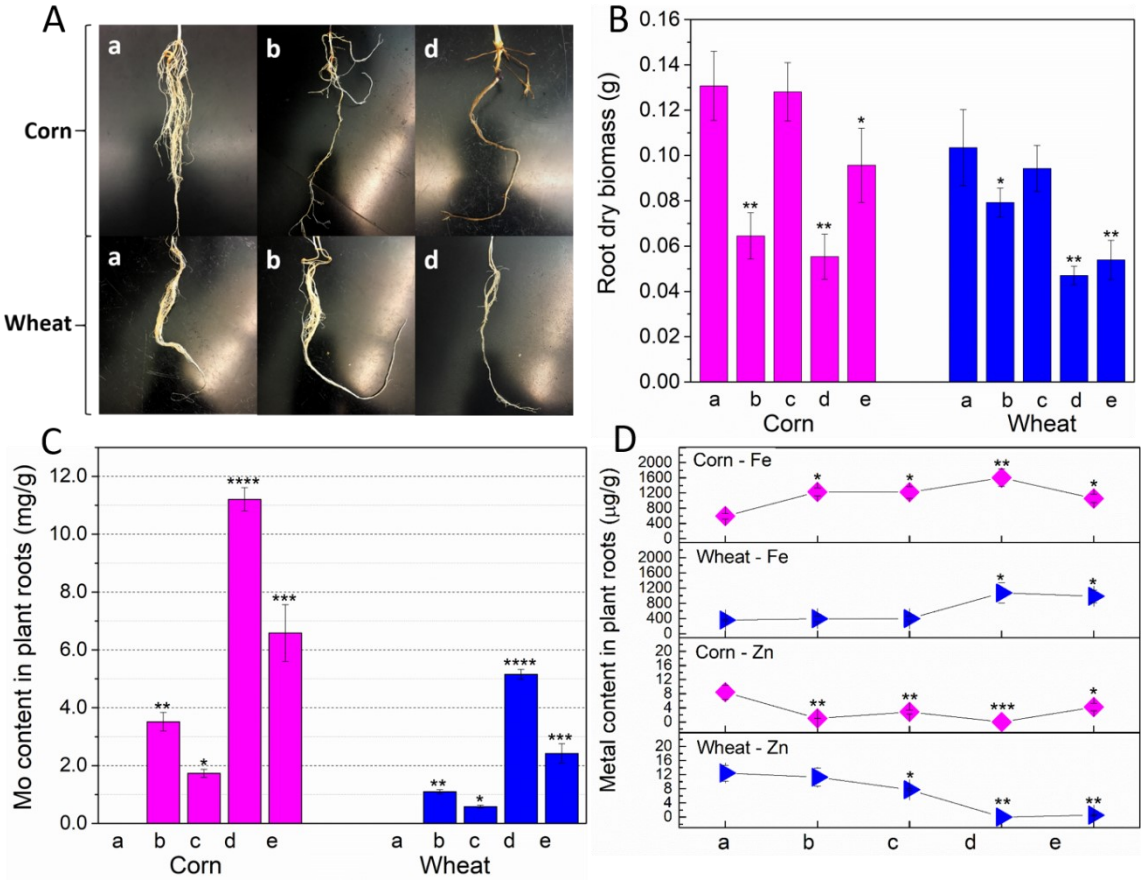

Figure 2. Corn and wheat root responses to MoO_3 NPs and ionic Mo. (A) Images of plant roots after three weeks of exposure at different doses; (B) dry biomass of plant roots; (C) Mo content detected in roots; and (D) significantly altered Fe and Zn levels. Treatment conditions: a. control group (no Mo added), b. 200 mg Mo NPs /kg vermiculite, c. 70 mg ionic Mo /kg vermiculite, d. 1000 mg Mo NPs /kg vermiculite, and e. 450 mg ionic Mo /kg vermiculite. Statistics based on a minimum of three replicates. Error bars represent the standard deviation. * indicates significant differences ($p < 0.05$) compared with the control (group a).

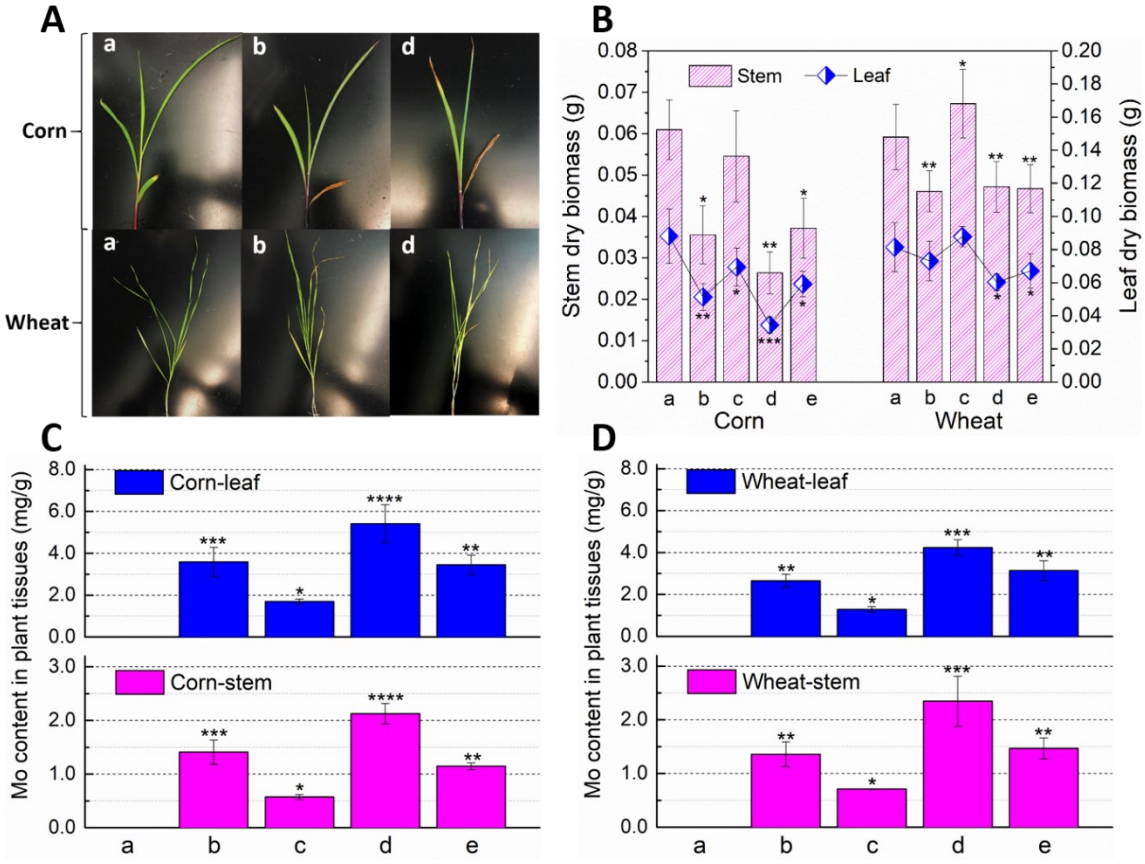

Figure 3. Corn and wheat stem and leaf responses to MoO_3 NPs and ionic Mo. (A) Images of plant stems and leaves after three weeks of root exposure at different doses; (B) dry biomass of plant stems and leaves; (C) Mo content in corn tissues; and (D) Mo content in wheat tissues. Treatment conditions: a. control group (no Mo added), b. 200 mg Mo NPs /kg vermiculite, c. 70 mg ionic Mo /kg vermiculite, d. 1000 mg Mo NPs /kg vermiculite, and e. 450 mg ionic Mo /kg vermiculite. Statistics based on a minimum of three replicates. Error bars represent the standard deviation. * indicates significant differences ($p < 0.05$) compared with the control (group a).

Root metabolomics of corn and wheat exposed to MoO_3 NPs and ionic Mo

Since the plants were exposed via the roots, and root tissues accumulated significant amounts of Mo (Figure 2C), the changes in metabolite levels were expected to be most noticeable in these tissues, particularly for corn. The overall PLS-DA analysis of the 82 metabolites clearly indicated separation of the control and the

300 treatments for corn roots (Figure 4A and Figure S1) and for wheat roots (Figure 5A and Figure S1). For
301 corn roots, there was also clear separation for the 200 mg/kg NP (treatment b) compared to the
302 corresponding 70 mg/kg ionic Mo (treatment c). However, the high-level exposures (treatments d and e)
303 for corn roots overlapped, indicating a similar metabolomics response. In the case of wheat roots, the
304 metabolite profiles separated well among different treatment conditions.
305 Analysis of individual metabolite groups yielded further insights. Since only one fatty acid was detected
306 in roots (linoleic acid), this group was not analyzed in detail. There was clear separation of antioxidants,
307 nucleic acids and organic acids between the control and the treatments in corn roots (Figures 4C - 4E),
308 indicating that in corn, these groups of metabolites are more sensitive to higher levels of Mo The levels of
309 amino acids and sugars also respond to Mo treatments in corn roots, except the 200 mg/kg MoO_3 NP
310 (treatment b) (Figures 4B and 4F). Given that corn exhibited a more marked physiological response to the
311 NP and ionic Mo treatments, it follows that the metabolic response would be generally significant for almost
312 all treatments. For wheat, the separation between control and treatments was clear for amino acids and
313 nucleic acids (Figures 5B and 5D), but the other groups of metabolites overlapped to some extent with the
314 control, in particular for antioxidants (Figure 5C). There was some separation between treatments for the
315 sugars, more distinctly for the high-level NP and ionic treatments (Figure 5F). The metabolomics responses
316 in roots correlated well with the Mo content in roots, where the higher Mo treatment groups (treatment d
317 and e) had 3.2-4.7 times more accumulated Mo than lower Mo exposure conditions (treatment b and c) and
318 the elevated Mo in plant roots resulting in clearer separations from the control group. From these analyses,
319 we began to infer that a more in-depth analysis could yield more insights.
320 By combining the statistical analysis (PLS-DA and ANOVA) of the individual metabolite groups, three
321 additional metabolites were identified as significantly dysregulated: benzoic acid, ornithine and raffinose
322 (Figure 6). Even though these three metabolites were not dysregulated in all root exposure treatments,
323 substantial changes were consistently observed at the high Mo NP dose (treatment d). Heat maps and
324 pathway analyses demonstrated that corn root metabolite profiles exhibited more substantial changes than
325 those of wheat roots (Figure S2-S5). The significantly accumulation of citric acid, malic acid, and succinic

326 acid in corn roots (Figure S4) indicated perturbation of the tricarboxylic acid (TCA) pathway, which is the
327 major pathway for energy resources and a key metabolic pathway related to many other important
328 biosynthesis intermediates (e.g., plant hormones and amino acids). Unlike corn roots, the TCA cycle in
329 wheat roots was barely perturbed, except that citric acid was slightly decreased (0.89 times as the control)
330 when exposed to Mo NPs (Figure S5). There were 15 pathways altered in corn roots versus only 2 pathways
331 significantly changed in wheat roots (Table S3). Ornithine was involved in one of the perturbed pathways
332 (glutathione metabolism) in wheat. It is worth noting that ornithine was overlooked by the overall
333 metabolite analysis, but was identified via the individual metabolite group analysis. Even though ornithine
334 is a non-essential amino acid, it participates in the central reactions of the urea cycle (Figure S5).
335
336
337
338

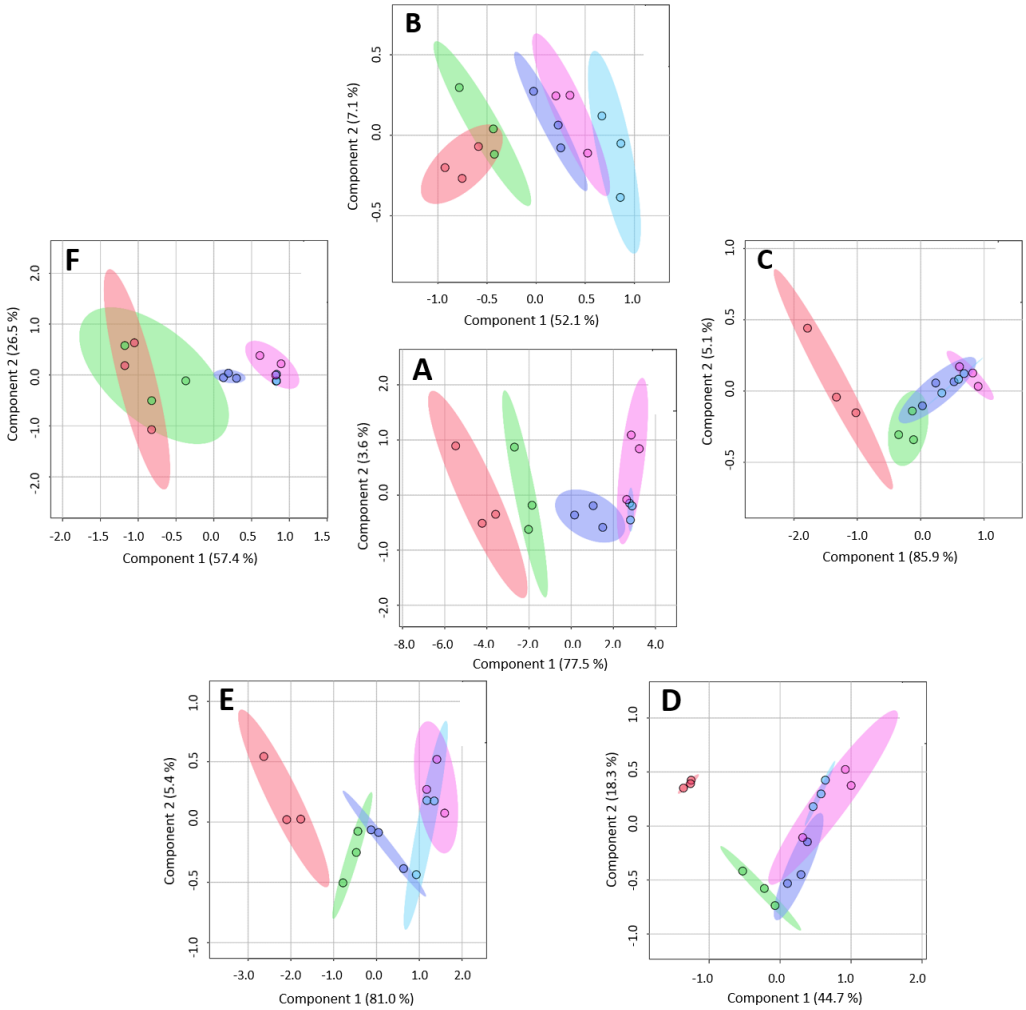

Figure 4. Partial least-squares discriminate analysis (PLS-DA) score plot of (A) the overall, (B) amino acids, (C) antioxidants, (D) nucleic acids, (E) organic acids, and (F) sugars metabolites profile in corn roots for different root Mo exposures. Symbols a-e represents different conditions: a (●) control group (no Mo added), b (●) 200 mg /kg MoO_3 NPs, c (●) 70 mg/kg Na_2MoO_4, d (●) 1000 mg/kg MoO_3 NPs, and e (●) 450 mg/kg Na_2MoO_4.

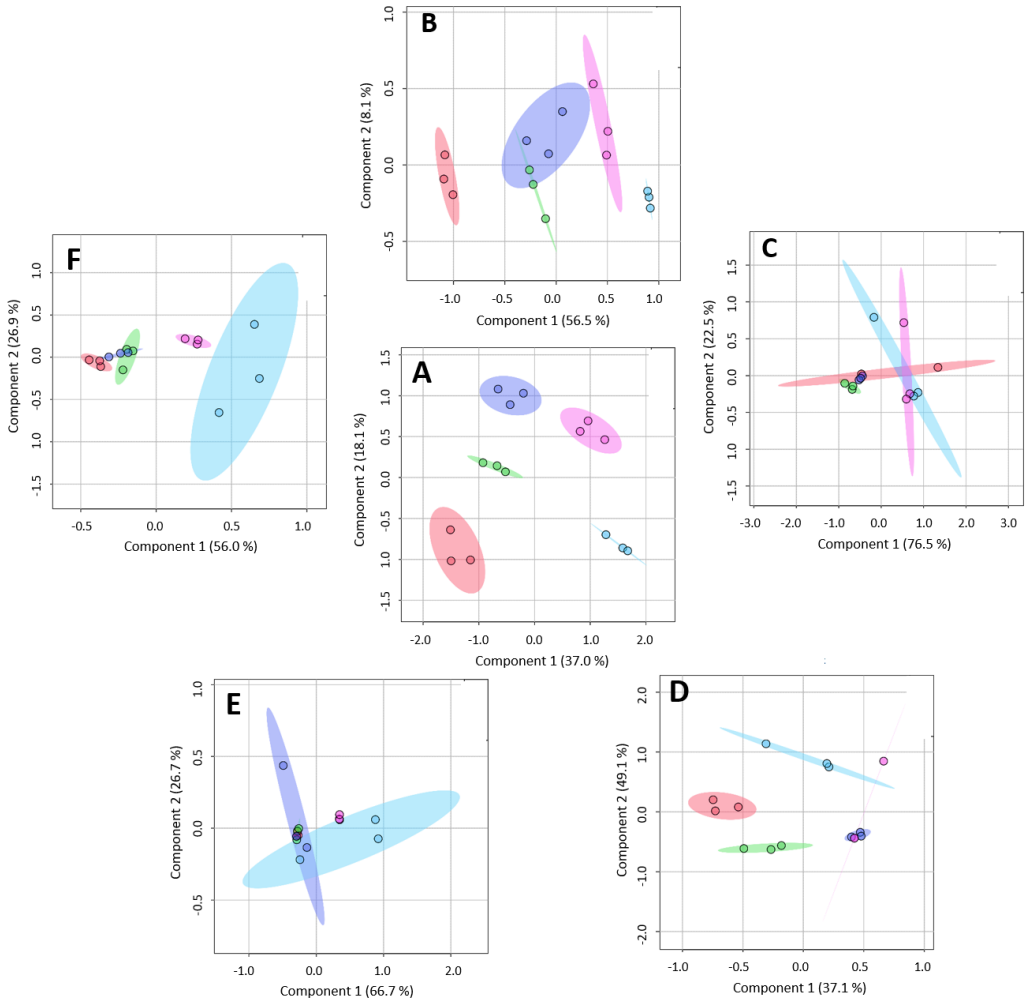

Figure 5. Partial least-squares discriminate analysis (PLS-DA) score plot of (A) the overall, (B) amino acids, (C) antioxidants, (D) nucleic acids, (E) organic acids, and (F) sugars metabolites profile in wheat roots for different root exposure. Symbols a-e represents different conditions: a (●) control group (no Mo added), b (●) 200 mg /kg MoO_3 NPs, c (●) 70 mg/kg Na_2MoO_4, d (●) 1000 mg/kg MoO_3 NPs, and e (●) 450 mg/kg Na_2MoO_4.

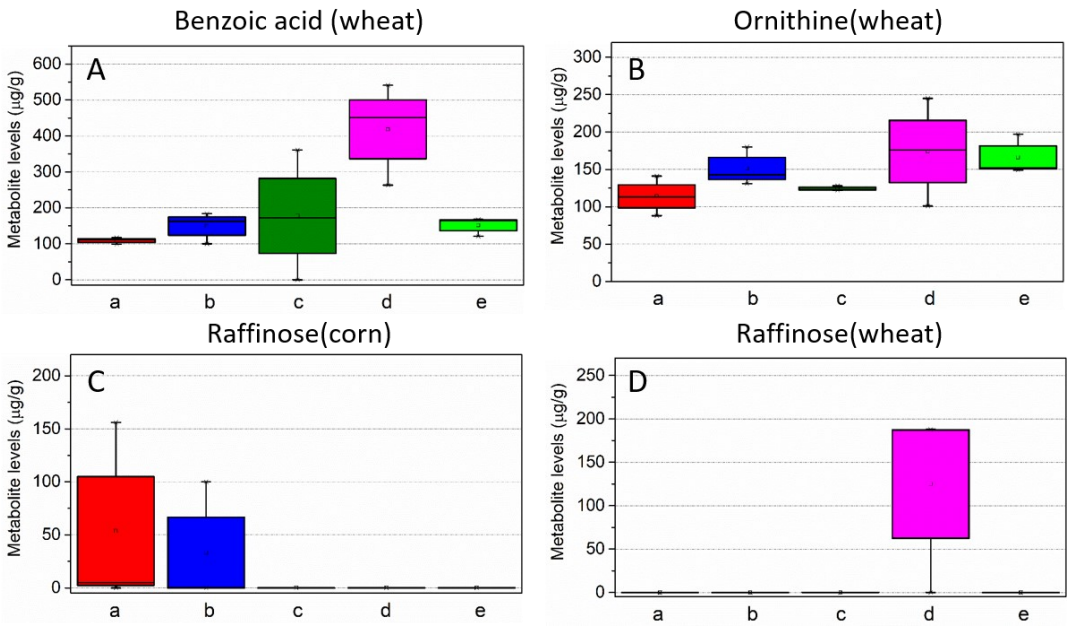

Figure 6. Box plot of metabolites with VIP score >1 that could only be detected when the individual metabolites categories were analyzed in corn and wheat roots. Treatment conditions: a. control group (no Mo added), b. 200 mg Mo NPs /kg vermiculite, c. 70 mg ionic Mo /kg vermiculite, d. 1000 mg Mo NPs /kg vermiculite, and e. 450 mg ionic Mo /kg vermiculite.

Leaf metabolomics of corn and wheat exposed to MoO_3 NPs and ionic Mo

The PLS-DA analysis of the overall set of metabolites in above-ground plant tissues (i.e., stems and leaves), in general indicated good separation between the control and exposure groups (Figures S6 and S7). Similar to the results of root metabolites, the higher Mo exposures usually led to larger separation with respect to the control. Given that a significant amount of Mo was translocated to plant stems (0.57-2.35 mg/g) and leaves (1.28-5.41 mg/g) (Figure 3C and 3D), significant metabolic reprogramming was hypothesized. Overall, 33 more metabolites were altered in corn roots (Figure S2) than corn leaves (Figure 7), showing the more extensive metabolite profile alteration in the direct-contact plant tissue sections. In addition, 21 metabolites were differentially expressed in corn leaves, of which 11 were identified by the overall metabolomics analysis. The additional 10 metabolites (circled in red in Figure 7) were only identified when an analysis by groups of metabolites was conducted. Since these 10 metabolites are generally expressed at much lower concentrations than those identified in the overall metabolomics analysis, their dysregulation

370 was difficult to discern, requiring additional analysis. Among them, glutamine and hypoxanthine were
371 involved in the perturbed purine metabolism and two other metabolites (arginine and ornithine) were
372 important metabolites in the perturbed arginine and proline metabolism pathway (Table S4). Glutamine is
373 the primary product of ammonium assimilation, which is a central metabolite in nitrogen metabolism [47].
374 The decreased glutamine levels in corn leaves indicates an altered ability to acquire N compounds. Elevated
375 hypoxanthine, along with other significantly changed metabolites (adenosine and guanine) indicates an
376 alteration of purine metabolism. Arginine serves to store nitrogen in plants and it is also the signaling
377 molecule in the synthesis of NO, polyamines, and potentially proline [48]. Even though there are only a few
378 physiological functions where ornithine is presumed to be involved, it is known as a key intermediate for
379 the biosynthesis of arginine, proline, polyamines, glutamate, and alkaloids [49].

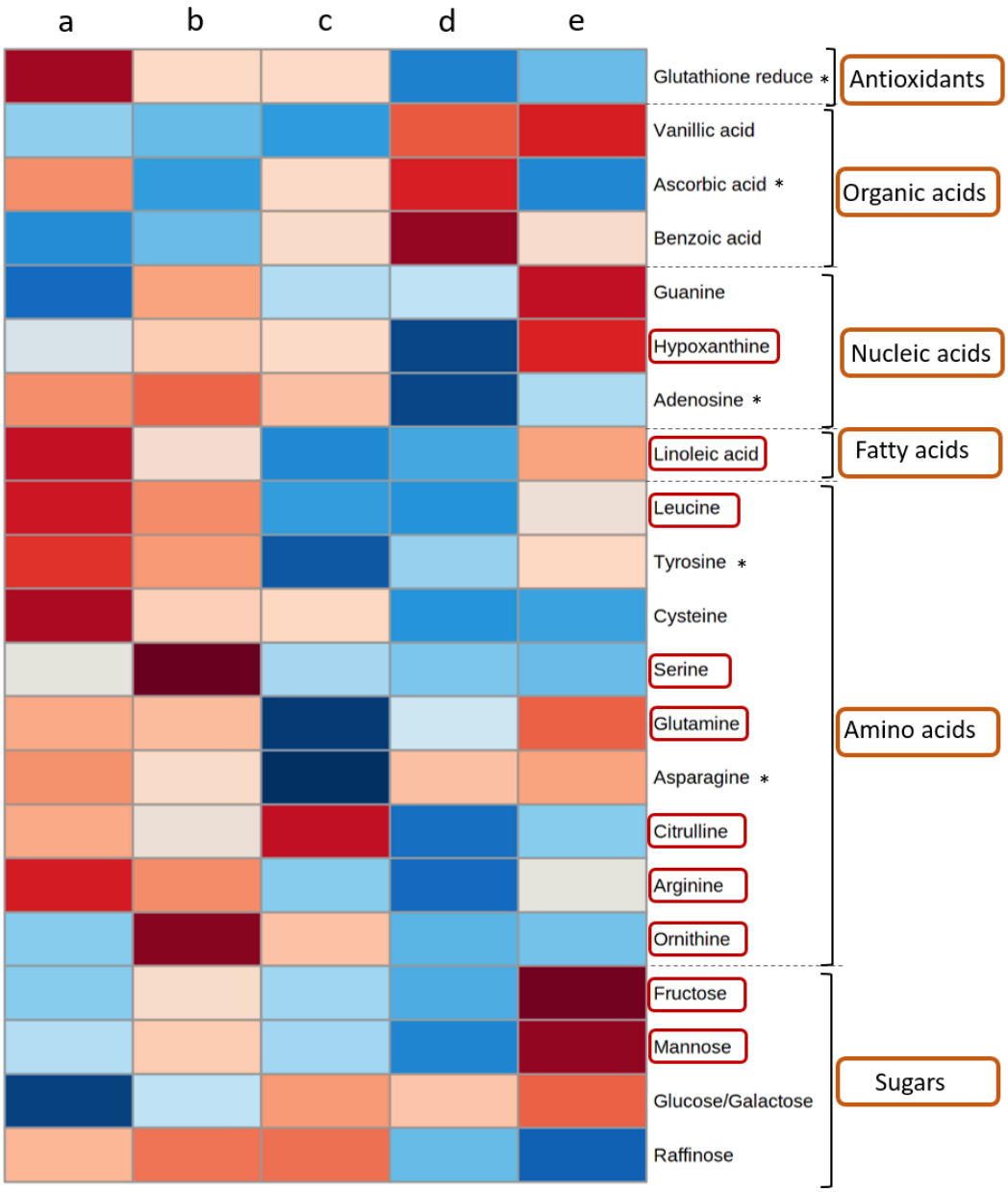

Figure 7. Heat map of corn leaf metabolites with altered levels after root exposure to MoO_3 NPs and ionic Mo. Color bar represents metabolites were from less abundant to more abundant. Metabolites circled in red could only be identified when the individual subcategories were analyzed. The asterisk indicates statistically significant differences (p-value < 0.05) in the overall metabolomics analysis. Treatment conditions: a. control group (no Mo added), b. 200 mg Mo NPs /kg vermiculite, c. 70 mg ionic Mo /kg vermiculite, d. 1000 mg Mo NPs /kg vermiculite, and e. 450 mg ionic Mo /kg vermiculite.

388 Surprisingly, metabolic reprograming in wheat leaves exposed to Mo NPs or ions was much more extensive
389 with 53 dysregulated metabolites (Figure 8). Six of the 53 altered metabolites were identified via the deeper
390 analysis, including several nucleic acids and sugars. This was unexpected since all the earlier data
391 (physiological response, changes in biomass, and accumulation of Mo) in wheat leaves indicated less
392 response from wheat leaves than corn leaves. Metabolite pathway analysis revealed that the metabolomic
393 profile was influenced more by Mo NP exposure in wheat leaves than in corn leaves (Figures S8 and S9).
394 Additional pathways that were perturbed in wheat leaves, but not in corn leaves, were TCA cycle, amino
395 acid metabolism, and pyrimidines metabolism. Six metabolites (adenine, adenosine, fructose, asparagine,
396 methionine, tyrosine) had unique responses to exposure to Mo NPs via wheat leaves, and only one
397 metabolite (adenosine) had the same response in corn leaves. It is worth noting that two of the newly
398 discovered metabolites (hypoxanthine and guanosine) from wheat leaves were involved in the significantly
399 perturbed purine metabolism (Figure 8 and Table S4 & S8). Clearly, there is a level of tolerance for Mo,
400 but at a higher dose it results in substantial metabolic reprogramming.
401 In summary (Table S5), although clear separation was observed in the overall metabolomics for all
402 treatments vs. the control, the separation can be more clearly attributed to different groups of metabolites,
403 with some variation in the response between the two plant species, as well as for the three tissues analyzed
404 (roots, stems and leaves). The deeper analysis of the metabolomics, going beyond the overall metabolomics
405 to the analysis of the response in individual groups of metabolites, proved useful in identifying additional
406 metabolites in plant tissues that responded to Mo root exposures (Figure 9). Summing up the metabolomics
407 analysis of roots, stems and leaves, 7 additional metabolites were discovered that were significantly altered
408 in all plant tissues for corn, and also in wheat (Figure 9, Table S6 and S7). From the individual group
409 analysis, asparagine, fructose, reduced glutathione, and mannose were found as metabolites that were
410 reprogrammed in both corn and wheat plant tissues (from root to leaf). Asparagine (combined with
411 glutamine and arginine), is a major nitrogen transporter and serves to fix N in plants. Thus, changes in
412 asparagine levels may affect the ability of the plant to synthesize N compounds, which could further affect
413 key building blocks of plant proteins and enzymes [50]. Glutathione plays a crucial role increasing plant

414 tolerance levels and providing efficient protection towards abiotic stress-induced ROS accumulation [51].
415 Fructose can be produced via glycolysis and it provides antioxidative properties that promoted plant
416 adaptation to cold weather [52]. Another simple polysaccharide, mannose, also has been reported to govern
417 the expression of the antioxidant defense system and to be significantly altered under cold [53] and
418 environmental (i.e., SiO_2, TiO_2, and Fe_3O_4) stressors [54]. These results are comparable to the metabolomics
419 of corn exposed to $Cu(OH)_2$ NPs [30, 34], where effects on several metabolic pathways (glycolytic pathway,
420 TCA cycle, and shikimate-phenylpropanoid biosynthesis) and other biosynthetic pathways (e.g., sugars,
421 amino acid, lipids) were observed. However, the key perturbed metabolites were different, indicating that
422 exposure to Mo (NPs and ionic solution) results in very different responses, compared to Cu NPs.

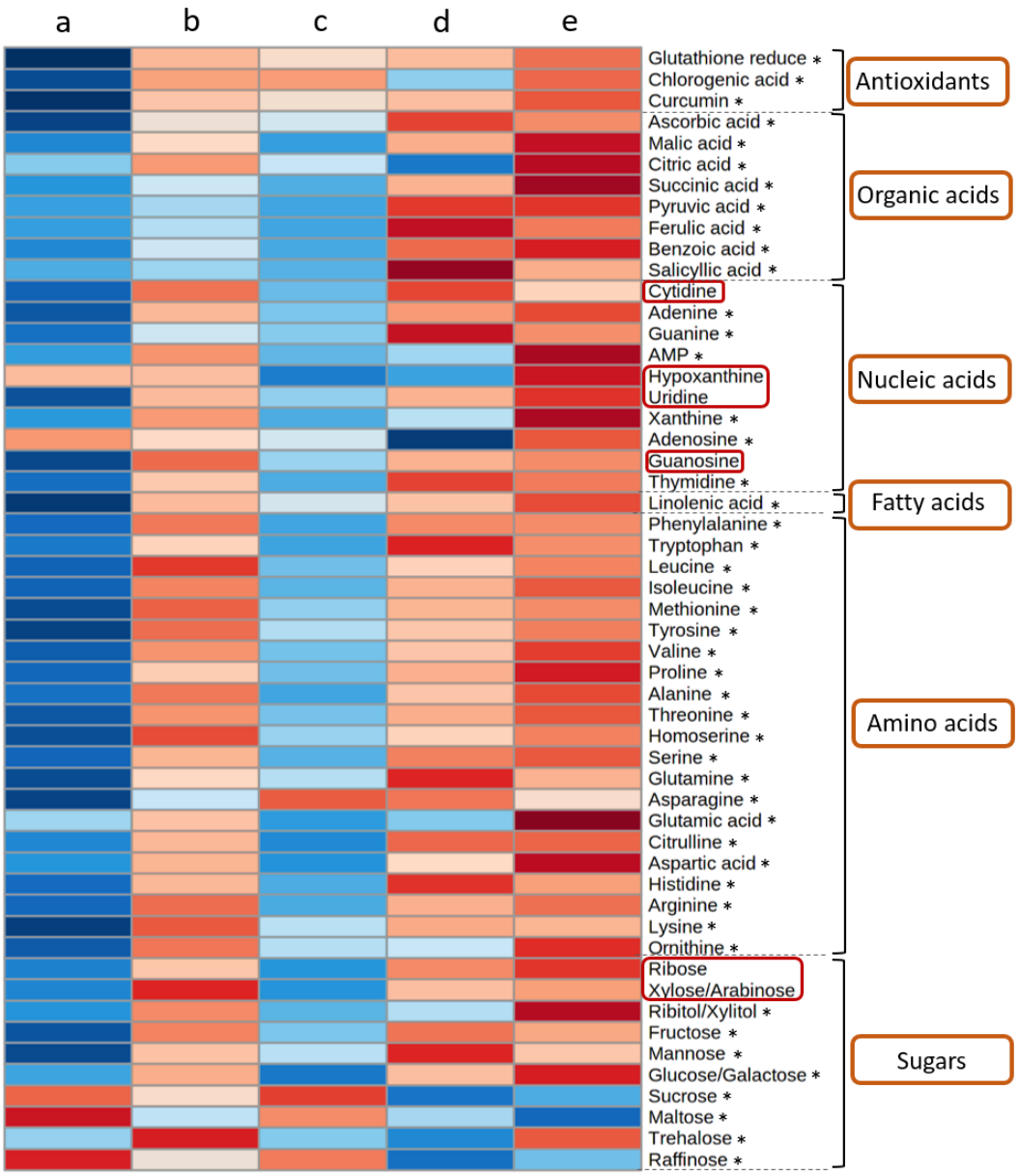

Figure 8. Heat map of wheat leaf metabolites with altered levels after root exposure to MoO_3 NPs and ionic Mo. Color bar represents metabolites were from less abundant to more abundant. Metabolites circled in red could only be identified when the individual subcategories were analyzed. The asterisk indicates statistically significant differences (p-value < 0.05) in the overall metabolomics analysis. Treatment conditions: a. control group (no Mo added), b. 200 mg Mo NPs /kg vermiculite, c. 70 mg ionic Mo /kg vermiculite, d. 1000 mg Mo NPs /kg vermiculite, and e. 450 mg ionic Mo /kg vermiculite.

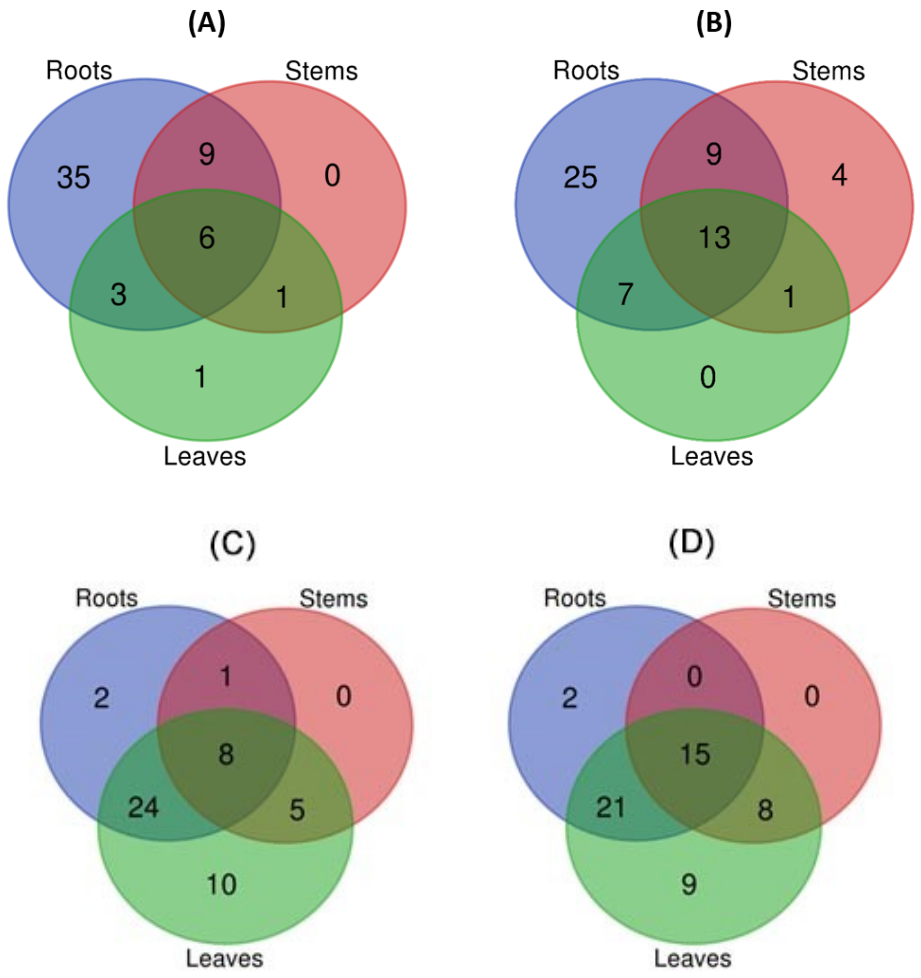

Figure 9 Venn diagram of important metabolites identified in (A) overall corn metabolomics and (B) individual metabolite groups for corn; and (C) overall wheat metabolomics and (D) individual metabolite groups for wheat.

Environmental Significance

The metabolomics of two important crops, corn and wheat, were evaluated after exposure to MoO_3 NPs and ionic Mo. The exposures were conducted at two levels, the lower one in the range of a hypothesized beneficial effect, and the higher one at a level expected to cause some effects on plant health. Physiologically, corn seedlings were more sensitive than wheat to Mo exposure in general, in either nano or ionic form, exhibiting yellowed leaves and reduced biomass. This likely is a reflection of the higher uptake and translocation of Mo by corn, compared to wheat. Surprisingly, the metabolomics of the wheat

exposures to Mo NPs and ions resulted in a dysregulation of more metabolites than corn. In leaves, most of the dysregulated metabolites in wheat exhibited up-regulation, for all Mo treatments. For corn, the pattern of dysregulation was less clear, with both up- and down-regulation of the altered metabolites. There was a clear differential effect between NP and ionic treatments, and plant responses were dose-dependent..

The deeper analysis of the metabolomics, considering different metabolite groups, yielded additional dysregulated metabolites, such as asparagine, fructose, reduced glutathione, and mannose. These results indicate a clear need to understand the benefits of Mo as a nanofertilizer, and to tailor the dose at a level that is beneficial for each crop plant, with minimal environmental implications. While this work focused on early-stage crop response to Mo NPs, full life cycle studies are recommended for future work to track the temporal dynamics in metabolite profiles. Additional omics (e.g. genomics, transcriptomics, proteomics) can also be used to further understand the response of plants to nanoagrochemicals and optimize the dose and timing of their application.

Supporting Information

The Supporting Information contains 7 tables and 9 figures, detailing the growth media, LC-MS/MS methods and analytes, and metabolomics of roots, stems and leaves, including a pathway analysis.

Conflict of interest

The authors declare no conflict of interest.

Acknowledgements

This work was supported by the National Science Foundation (NSF) under cooperative agreement number NSF-1901515. Arturo A. Keller also appreciates Agilent Technologies for their Agilent Thought Leader Award. Pabel Cervantes-Aviles thanks CONACYT. We also thank Dr. Sanghamitra Majumdar for her advice on the experimental approach, and Arthur Kao, Devin Everett and Xiaofan Liu for their contributions to the experimental work.

References

469 (1) Majumdar, S. and Keller, A. A. Omics to address the opportunities and challenges of
470 nanotechnology in agriculture. *Crit. Rev. Environ. Sci. Technol.* **2020**, 18–42.

471 (2) Johnson, C. H.; Ivanisevic, J.; Siuzdak, G. Metabolomics: Beyond biomarkers and towards
472 mechanisms. *Nat. Rev. Mol. Cell Bio*. **2016**, *17* (7), 451–459.

473 (3) Wishart, D. S. Metabolomics for investigating physiological and pathophysiological processes.
474 *Physiol. Rev.* **2019**, *99* (4), 1819–1875.

475 (4) Powers, R. and Riekeberg, E. New frontiers in metabolomics: From measurement to insight.
476 *F1000Res*. **2017**, *6*.

477 (5) Kumar, R.; Bohra, A.; Pandey, A. K.; Pandey, M. K.; Kumar, A. Metabolomics for plant
478 improvement: Status and prospects. *Front. Plant Sci*. **2017**, *8*, 1302.

479 (6) Sharma, K.; Sarma, S.; Bohra, A.; Mitra, A.; Sharma, N. K.; Kumar, A. Plant Metabolomics: An
480 Emerging Technology for Crop Improvement. *New Vis. in Plant Sci*. **2018**, 65–79.

481 (7) Gomez, A.; Narayan, M.; Zhao, L.; Jia, X.; Bernal, R. A.; Lopez-Moreno, M. L.; Peralta-Videa, J.
482 R. Effects of nano-enabled agricultural strategies on food quality: Current knowledge and future
483 research needs. *J. Hazard. Mater*. **2021**, *401*, 123385..

484 (8) Kah, M.and Hofmann, T. Nanopesticide research: Current trends and future priorities. *Environ.*
485 *Int*. **2014**, *63*, 224–235.

486 (9) Giraldo, J. P.; Wu, H.; Newkirk, G. M.; Kruss, S. Nanobiotechnology approaches for engineering
487 smart plant sensors. *Nat. Nanotechnol*. **2019**, *14*, 541–553.

488 (10) Kah, M.; Kookana, R. S.; Gogos, A.; Bucheli, T. D. A critical evaluation of nanopesticides and
489 nanofertilizers against their conventional analogues. *Nat. nanotechnol.* **2018,** *13*, 677-684.

490 (11) C Gupta, U.; C Srivastava, P.; C Gupta, S. Role of micronutrients: Boron and molybdenum in

491 crops and in human health and nutrition. *Curr. Nutr. & Food Sci.* **2011,** *7* (2), 126-136.

492 (12) Maillard, A.; Etienne, P.; Diquélou, S.; Trouverie, J.; Billard, V.; Yvin, J.-C.; Ourry, A. Nutrient
493 deficiencies modify the ionomic composition of plant tissues: a focus on cross-talk between
494 molybdenum and other nutrients in *Brassica napus*. *J. Exp. Bot.* **2016**, *67* (19), 5631–5641.

495 (13) Kovács, B.; Puskás-Preszner, A.; Huzsvai, L.; Lévai, L.; Bódi, É. Effect of molybdenum treatment
496 on molybdenum concentration and nitrate reduction in maize seedlings. *Plant Physiol. Biochem.*
497 **2015**, *96*, 38–44.

498 (14) Hewitt, E. J. and Bolle-Jones, E. W. Molybdenum as a Plant Nutrient: II. The Effects of
499 Molybdenum Deficiency on Some Horticultural and Agricultural Crop Plants in Sand Culture. *J.*
500 *Hortic. Sci.* **1952**, *27* (4), 257–265.

501 (15) Kaiser, B. N.; Gridley, K. L.; Ngaire Brady, J.; Phillips, T.; Tyerman, S. D. The Role of
502 Molybdenum in Agricultural Plant Production. *Ann. Bot.* **2005**, *96* (5), 745–754.

503 (16) Agarwala, S. C.; Sharma, C. P.; Farooq, S.; Chatterjee, C. Effect of molybdenum deficiency on the
504 growth and metabolism of corn plants raised in sand culture. *Can. J. Bot.* **1978**, *56* (16), 1905–
505 1908.

506 (17) Reddy, M. M.; Padmaja, B.; Malathi, S.; Rao, L. J. Effects of micronutrients on growth and yield
507 of pigeonpea. *J. SAT Agric. Res*. **2007**, *5* (1).

508 (18) Adhikari, T.; Kundu, S.; Rao, A. S. Impact of SiO 2 and Mo Nano Particles on Seed Germination
509 of Rice (Oryza Sativa L.). *Int. J. Food Sci. Tech.* **2013**, *4* (9), 2249–3050.

510 (19) Kanneganti, A. and Talasila, M. MoO_3 Nanoparticles: Synthesis, Characterization and Its
511 Hindering Effect on Germination of Vigna Unguiculata Seeds. *J. Eng. Res. Appl.* **2014**, *4* (7), 116–
512 120.

513 (20) Mushinskiy, A. A. and Aminova, E. V. Effect of iron, copper and molybdenum nanoparticles on

514 morphometric parameters of Solanum tuberosum L. plants. *IOP Conf. Ser. Earth Environ. Sci.*
515 **2019**, *341* (1), 012195.

516 (21) Abbasifar, A.; ValizadehKaji, B.; Iravani, M. A. Effect of green synthesized molybdenum
517 nanoparticles on nitrate accumulation and nitrate reductase activity in spinach. *J. Plant Nutr.* **2020**,
518 *43* (1), 13–27.

519 (22) Sharma, P. K.; Raghubanshi, A. S.; Shah, K. Examining the uptake and bioaccumulation of
520 molybdenum nanoparticles and their effect on antioxidant activities in growing rice seedlings.
521 *Environ. Sci. Pollut. Res.* **2021**, *28*, 13439-13453.

522 (23) Fadeel, B.; Farcal, L.; Hardy, B.; Vázquez-Campos, S.; Hristozov, D.; Marcomini, A.; Lynch, I.;
523 Valsami-Jones, E.; Alenius, H.; Savolainen, K. Advanced tools for the safety assessment of
524 nanomaterials. *Nat. Nanotechnol.* **2018**, *13* (7), 537–543.

525 (24) Olkhovych, O.; Volkogon, M.; Taran, N.; Batsmanova, L.; Kravchenko, I. The Effect of Copper
526 And Zinc Nanoparticles on the Growth Parameters, Contents of Ascorbic Acid, and Qualitative
527 Composition of Amino Acids and Acylcarnitines in Pistia stratiotes L. (Araceae). *Nanoscale Res.*
528 *Lett.* **2016**, *11*, 218.

529 (25) Hildebrandt, T. M.; Nesi, A. N.; Araújo, W. L.; Braun, H.-P. Amino acid catabolism in plants.
530 *Mol. Plant*. **2015,** *8*, (11), 1563-1579.

531 (26) Zhao, L.; Huang, Y.; Paglia, K.; Vaniya, A.; Wancewicz, B.; Keller, A. A. Metabolomics Reveals
532 the Molecular Mechanisms of Copper Induced Cucumber Leaf (Cucumis sativus) Senescence.
533 *Environ. Sci. Technol.* **2018**, *52* (12), 7092–7100.

534 (27) Zhao, L.; Huang, Y.; Adeleye, A. S.; Keller, A. A. Metabolomics Reveals Cu(OH)2
535 Nanopesticide-Activated Anti-oxidative Pathways and Decreased Beneficial Antioxidants in
536 Spinach Leaves. *Environ. Sci. Technol.* **2017**, *51* (17), 10184–10194.

537 (28) Zhao, L.; Huang, Y.; Hannah-Bick, C.; Fulton, A. N.; Keller, A. A. Application of metabolomics
538 to assess the impact of Cu(OH)2 nanopesticide on the nutritional value of lettuce (Lactuca sativa):
539 Enhanced Cu intake and reduced antioxidants. *NanoImpact*. **2016**, *3–4*, 58–66.

540 (29) Zhao, L.; Hu, Q.; Huang, Y.; Keller, A. A. Response at Genetic, Metabolic, and Physiological
541 Levels of Maize (Zea mays) Exposed to a Cu(OH)2 Nanopesticide. *ACS Sustain. Chem. Eng.*
542 **2017**, *5* (9), 8294–8301.

543 (30) Zhao, L.; Huang, Y.; Keller, A. A. Comparative Metabolic Response between Cucumber
544 (Cucumis sativus) and Corn (Zea mays) to a Cu(OH)2 Nanopesticide. *J. Agric. Food Chem.* **2018**,
545 *66* (26), 6628–6636.

546 (31) Tan, W.; Gao, Q.; Deng, C.; Wang, Y.; Lee, W. Y.; Hernandez-Viezcas, J. A.; Peralta-Videa, J.
547 R.; Gardea-Torresdey, J. L. Foliar Exposure of Cu(OH)2 Nanopesticide to Basil (Ocimum
548 basilicum): Variety-Dependent Copper Translocation and Biochemical Responses. *J. Agric. Food*
549 *Chem.* **2018**, *66* (13), 3358–3366.

550 (32) Zhang, H.; Du, W.; Peralta-Videa, J. R.; Gardea-Torresdey, J. L.; White, J. C.; Keller, A.; Guo, H.;
551 Ji, R.; Zhao, L. Metabolomics Reveals How Cucumber (Cucumis sativus) Reprograms Metabolites
552 to Cope with Silver Ions and Silver Nanoparticle-Induced Oxidative Stress. *Environ. Sci. Technol.*
553 **2018**, *52* (14), 8016–8026.

554 (33) Zhao, L.; Huang, Y.; Hu, J.; Zhou, H.; Adeleye, A. S.; Keller, A. A. 1H NMR and GC-MS Based
555 Metabolomics Reveal Defense and Detoxification Mechanism of Cucumber Plant under Nano-Cu
556 Stress. *Environ. Sci. Technol.* **2016**, *50* (4), 2000–2010.

557 (34) Zhao, L.; Huang, Y.; Zhou, H.; Adeleye, A. S.; Wang, H.; Ortiz, C.; Mazer, S. J.; Keller, A. A.
558 GC-TOF-MS based metabolomics and ICP-MS based metallomics of cucumber (: Cucumis
559 sativus) fruits reveal alteration of metabolites profile and biological pathway disruption induced by
560 nano copper. *Environ. Sci. Nano.* **2016**, *3* (5), 1114–1123.

561 (35) Majumdar, S.; Pagano, L.; Wohlschlegel, J. A.; Villani, M.; Zappettini, A.; White, J. C.; Keller, A.
562 A. Proteomic, gene and metabolite characterization reveal the uptake and toxicity mechanisms of
563 cadmium sulfide quantum dots in soybean plants. *Environ. Sci. Nano.* **2019**, *6* (10), 3010–3026.

564 (36) Huang, Y.; Li, W.; Minakova, A. S.; Anumol, T.; Keller, A. A. Quantitative analysis of changes in
565 amino acids levels for cucumber (Cucumis sativus) exposed to nano copper. *NanoImpact*. **2018**,
566 *12*, 9–17.

567 (37) Huang, Y.; Adeleye, A. S.; Zhao, L.; Minakova, A. S.; Anumol, T.; Keller, A. A. Antioxidant
568 response of cucumber (Cucumis sativus) exposed to nano copper pesticide: Quantitative
569 determination via LC-MS/MS. *Food Chem.* **2019**, *270*, 47–52.

570 (38) Liu, W.; Majumdar, S.; Li, W.; Keller, A. A.; Slaveykova, V. I. Metabolomics for early detection
571 of stress in freshwater alga Poterioochromonas malhamensis exposed to silver nanoparticles. *Sci.*
572 *Rep.* **2020**, *10* (1), 20563.

573 (39) Majumdar, S.; Ma, C.; Villani, M.; Zuverza-Mena, N.; Pagano, L.; Huang, Y.; Zappettini, A.;
574 Keller, A. A.; Marmiroli, N.; Dhankher, O. P.; White, J. C. Surface coating determines the
575 response of soybean plants to cadmium sulfide quantum dots. *NanoImpact*. **2019**, *14*, 100151.

576 (40) Scheffer, F. and Schachtschabel, P. Textbook of soil science. *Soil Sci.* Ferdinand Enke. **1982**.

577 (41) Shi, Z.; Zhang, J.; Wang, F.; Li, K.; Yuan, W.; Liu, J. Arbuscular mycorrhizal inoculation
578 increases molybdenum accumulation but decreases molybdenum toxicity in maize plants grown in
579 polluted soil. *RSC adv.* **2018,** *8* (65), 37069-37076.

580 (42) Cervantes-Avilés, P.; Huang, X.; Keller, A. A. Effectiveness of nanoagrochemical application:
581 Dissolution and aggregation of metal oxide nanoparticles in root exudates and soil leachate. *Rev.*
582 **2021**.

583 (43) Hong, J.; Peralta-Videa, J. R.; Rico, C.; Sahi, S.; Viveros, M. N.; Bartonjo, J.; Zhao, L.; Gardea-

584 Torresdey, J. L. Evidence of translocation and physiological impacts of foliar applied CeO2
585 nanoparticles on cucumber (Cucumis sativus) plants. *Environ. Sci. Technol.* **2014**, *48* (8), 4376–
586 4385.

587 (44) Zhao, L.; Hu, Q.; Huang, Y.; Fulton, A. N.; Hannah-Bick, C.; Adeleye, A. S.; Keller, A. A.
588 Activation of antioxidant and detoxification gene expression in cucumber plants exposed to a
589 Cu(OH)2 nanopesticide. *Environ. Sci. Nano.* **2017**, *4* (8), 1750–1760.

590 (45) Aubert, T.; Burel, A.; Esnault, M.-A.; Cordier, S.; Grasset, F.; Cabello-Hurtado, F. Root uptake
591 and phytotoxicity of nanosized molybdenum octahedral clusters. *J. Hazard. Mater.* **2012,** *219*,
592 111-118.

593 (46) Müller, C.; Elliott, J.; Levermann, A. Fertilizing hidden hunger. *Nat. Clim. Change*. **2014,** *4* (7),
594 540-541.

595 (47) Chellamuthu, V.-R.; Ermilova, E.; Lapina, T.; Lüddecke, J.; Minaeva, E.; Herrmann, C.;
596 Hartmann, M. D.; Forchhammer, K. A widespread glutamine-sensing mechanism in the plant
597 kingdom. *Cell*. **2014,** *159* (5), 1188-1199.

598 (48) Winter, G.; Todd, C. D.; Trovato, M.; Forlani, G.; Funck, D. Physiological implications of
599 arginine metabolism in plants. *Front. Plant Sci.* **2015,** *6*, 534.

600 (49) Majumdar, R.; Minocha, R.; Minocha, S. Ornithine: at the crossroads of multiple paths to amino
601 acids and polyamines. *In: D'Mello, JPF, ed. Amino acids in higher plants.* Osfordshire, UK:
602 CABI: 156-176. Chapter 9. **2015**, 156-176.

603 (50) Lea, P. J.; Sodek, L.; Parry, M. A.; Shewry, P. R.; Halford, N. G. Asparagine in plants. *Ann. Appl.*
604 *Biol.* **2007,** *150* (1), 1-26.

605 (51) Gallé, Á.; Czékus, Z.; Bela, K.; Horváth, E.; Ördög, A.; Csiszár, J.; Poór, P. Plant glutathione
606 transferases and light. *Front. Plant Sci.* **2019,** *9*, 1944.

607 (52) Bogdanović, J.; Mojović, M.; Milosavić, N.; Mitrović, A.; Vučinić, Ž.; Spasojević, I. Role of
608 fructose in the adaptation of plants to cold-induced oxidative stress. *Eur. Biophys. J.* **2008,** *37* (7),
609 1241-1246.

610 (53) Chai, F.; Liu, W.; Xiang, Y.; Meng, X.; Sun, X.; Cheng, C.; Liu, G.; Duan, L.; Xin, H.; Li, S.
611 Comparative metabolic profiling of Vitis amurensis and Vitis vinifera during cold acclimation.
612 *Hortic. Res.* **2019,** *6*, 8.

613 (54) Zhao, L.; Zhang, H.; White, J. C.; Chen, X.; Li, H.; Qu, X.; Ji, R. Metabolomics reveals that
614 engineered nanomaterial exposure in soil alters both soil rhizosphere metabolite profiles and maize
615 metabolic pathways. *Environ. Sci.: Nano*. **2019,** *6* (6), 1716-1727.

616

617

618

619

620

621

622

623

624

625